http://www.aimspress.com/journal/Materials

*Research article*

# Characterization of the mechanical properties and thermal conductivity of epoxy-silica functionally graded materials

**Jaafar Sh. AbdulRazaq[1,\*], Abdul Kareem F. Hassan[1] and Nuha H. Jasim[2]**

[1] Department of Mechanical Engineering, College of Engineering, University of Basrah, Basrah, Iraq

[2] Department of Materials Engineering, College of Engineering, University of Basrah, Basrah, Iraq

**\* Correspondence:** Email: engpg.jaafar.shreef@uobasrah.edu.iq; Tel: +9647802262926.

**Abstract:** A functionally graded material (FGM) was prepared using epoxy resin reinforced with silicon dioxide with a particle size of 100 μm and weight percentages of 0, 20, 40, 60, and 80 wt%. In a gravity-molding process using the hand layup technique, specimens with international standard (ASTM)-calculated dimensions were created in a mold of poly(methyl methacrylate), which is also known as acrylic. Tensile, flexural, impact, infrared wave, and thermal conductivity tests, and X-ray diffraction (XRD) were conducted on specimens of the five layers of the FGM. The XRD and infrared spectroscopy demonstrated that the compositions of the silica particles and epoxy had a strong association with their physical structures. The findings of experimental tests indicated that increasing the ratio of silicon dioxide enhanced the mechanical properties, and the increase in modulus of elasticity was directly related to the weight percentage of the reinforcement material. The composite with 80% silica had a 526.88% higher modulus of elasticity than the pure epoxy specimen. Both tensile and flexural strengths of the composite material were maximal when 40 wt% of the particle silicon dioxide was utilized, which were 68.5% and 67.8% higher than those of the neat epoxy, respectively. The test results also revealed that the impact resistance of the FGM increased when the silica proportion increased, with a maximum value of 60 wt% silica particle content, which was an increase of 76.98% compared to pure epoxy. In addition, the thermal properties of epoxy resin improved when $SiO_2$ was added to the mixture. Thus, the addition of silica filler to composite materials directly proportionally increased their thermal conductivity to the weight ratio of the reinforcement material, which was 32.68–383.66%. FGM composed of up to 80% silica particles had the highest thermal conductivity.

## 1. Introduction

Functionally graded materials (FGMs) are a class of composite materials that have been manufactured by a unique process to achieve impossible properties with monolithic materials and perform better than traditional composites [1]. In general, two types of property gradients result from the manufacturing process: stepwise and continuous [2]. FGM concepts are gaining importance in several fields of material science, and the pressing necessity of practical application of materials has generated additional requirements. FGMs can address and resolve issues that result from the development and application of advanced composite materials [3].

In the field of advanced engineered materials, polymer matrix composites are utilized in various industrial applications due to their unique benefits, which include simplicity of manufacturing, light weight, ductility, and relatively low cost [4]. The matrix consists of thermoplastic polymers and thermosetting resins [5]. Polymer composites have been intensively studied for a long time; inorganic fillers predominantly fill these organic polymer composites, and their characteristics include those of the inorganic filler material (toughness and thermal stability) and organic polymer (ductility, flexibility, and processability) [6–8]. Shen and Bever studied polymer composite gradients [9]. They began their research on the structures and properties of polymer materials with spatial gradients and expressed interest in potential applications of these materials. Mulugeta et al. [10] mentioned that fillers such as clay, silica, glass, or carbon fiber could improve the toughness and often perform in synergy with elastomeric toughness.

In various studies, silica fillers enhanced the mechanical properties, including the modulus, strength, and stiffness. However, the characteristics of the composites were uniformly distributed throughout the materials and produced homogeneous products [11]. Thus, many applications necessitate the use of FGMs, which mechanically outperform conventional composites with homogeneous compositions [12]. FGM designs focus on certain desired traits of each constituent material. For instance, silica may be utilized on the hotter side of the FGM specimen and polymer on the cooler side to benefit from the higher mechanical and heat transmission qualities of each material [13,14]. Consequently, to mitigate problems caused by an abrupt change in thermomechanical characteristics, e.g., in the case of composite materials, and to obtain the necessary qualities, FGMs are heterogeneous composites where the material properties gradually vary between two surfaces [15]. In other words, FGMs can be described as composites where the material characteristics gradually change along a certain direction as a function of the appropriate attributes [16].

FGMs with polymer and ceramic components are commonly known for improving mechanical and thermal characterization due to the seamless transition between the components' characteristics [17]. In this paper, epoxy-silica FGMs are studied, and certain distinctions between graded and composite materials are discussed. Thermal conductivity and mechanical property tests were performed on an FGM specimen and the five layers of its functional gradation. The outcomes will help readers understand that FGMs can solve practical issues that arise from the production and application of innovative types of polymer-based composites with polymer ceramic combinations to improve their properties via gradation in epoxy-silica composition. We hope that our findings will

help researchers who are interested in the science and engineering of gradient materials for epoxy-silica compositions.

## 2. Materials and methods

### 2.1. Preparation of FGM specimens

The polymer utilized was an epoxy resin with low viscosity. Silicon dioxide ($SiO_2$) powder with a particle size of 100 μm was used as the filler material in the epoxy matrix to prepare stepwise FGMs. An FGM sample consisting of five layers of graded epoxy-silica was prepared using the hand layup technique and poured into a mold made of poly(methyl methacrylate), which is also known as acrylic, with internal dimensions of 270 mm $\times$ 170 mm $\times$ 10 mm. This process is shown in Figure 1.
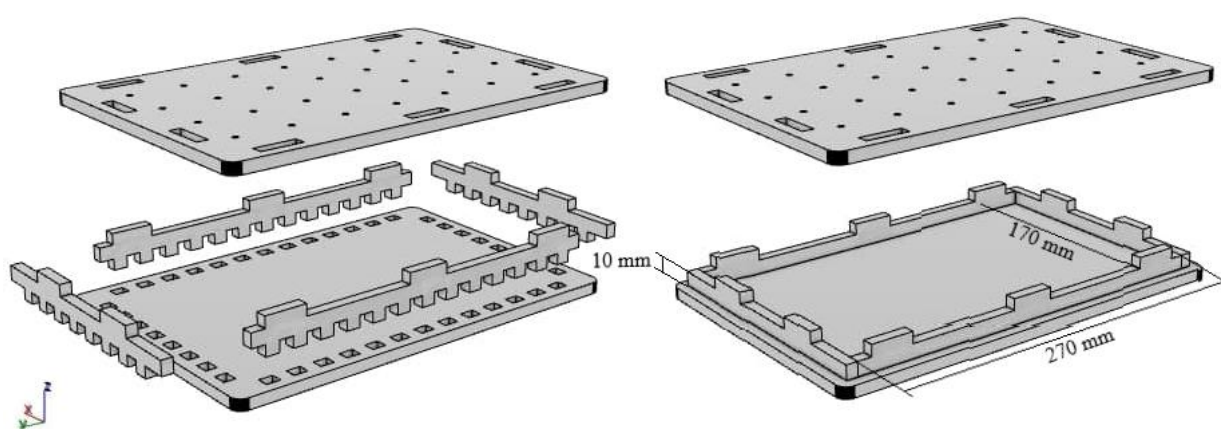


**Figure 1.** Design of an acrylic mold in the Autodesk 3Ds Max program.

The mold was created using a computer numerical control (CNC)/laser/plasma machine to cut an acrylic transparent sheet (8 mm) into six pieces according to the given dimensions. Then, the mold parts were assembled, and a gradient scale was added to the side parts of the acrylic mold every 2 mm to show the height level for each layer of stepwise FGM during the manufacturing process. A mold release agent (honey wax) was utilized to coat the mold's joints to prevent the composite from leaking out of the mold during the pouring process, avoid sticking, and facilitate the elicitation of the FGM sample [18–20]. As shown in Table 1, the FGM was manufactured according to a weight gradient for each layer, where the epoxy resin was mixed with varying amounts of silicon dioxide (0, 20, 40, 60, and 80 wt%). At room temperature, the material was manually mixed with a glass rod until it was homogeneous; then, it was poured into the mold in a gravity-molding process using the hand layup technique [21,22]. The FGM generated using this step-by-step casting approach was formed by pouring resin with varying filler volume contents in succession [23,24]. The mold was partially filled with the first layer of pure epoxy; then, the second layer of epoxy, which was mixed with a specific volume of silicon dioxide, was poured on top of the partially solidified first layer. The layers were arranged from 0–80 wt% silicon dioxide. When the layers were complete, the mold cover was placed on top to obtain a homogenous thickness. Figure 2 depicts a model of the stepwise FGM profile. In addition to the five-layer graduated sample, five additional samples that

represented each layer of the graduated sample were prepared to examine and identify the characteristics of each layer in the graded sample.

**Table 1.** Model of the FGM profile.

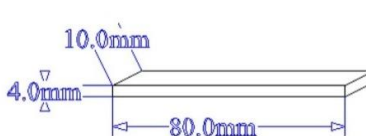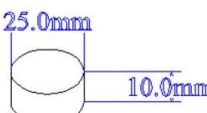| Layer no. | Percentage of layer composition | Layer thickness (mm) | Weight mixture of epoxy (g) | Weight of silica (g) | Nomenclature |
| --- | --- | --- | --- | --- | --- |
| 1 | 100% epoxy | 2 | 96.39 | 0 | Ep1 |
| 2 | 80% epoxy, 20% silica | 2 | 77.11 | 24.42 | Ep/S2 |
| 3 | 60% epoxy, 40% silica | 2 | 57.83 | 48.84 | Ep/S3 |
| 4 | 40% epoxy, 60% silica | 2 | 38.56 | 73.26 | Ep/S4 |
| 5 | 20% epoxy, 80% silica | 2 | 19.28 | 97.68 | Ep/S5 |
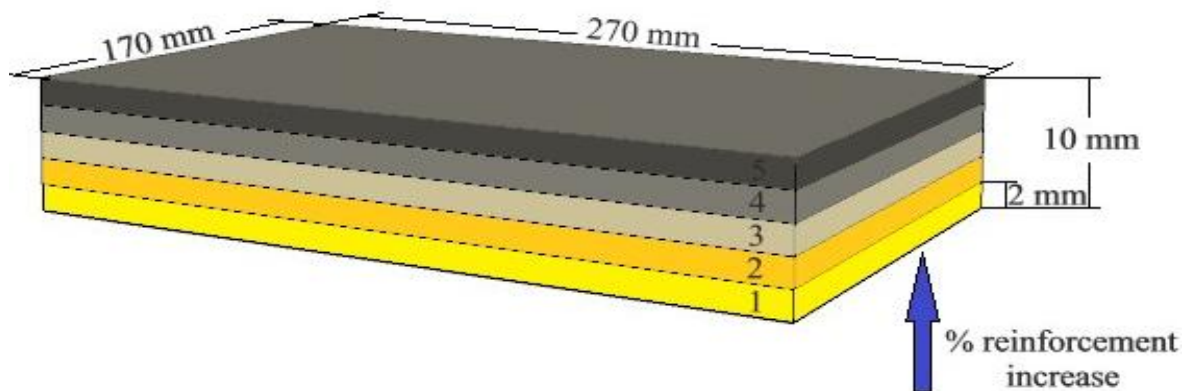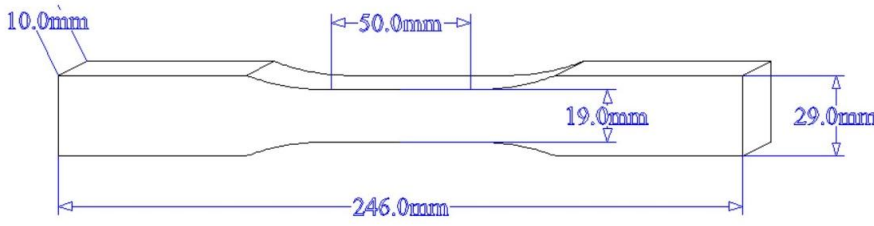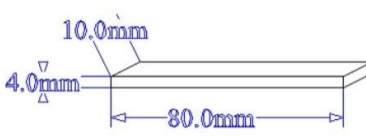


**Figure 2.** Five layers of stepwise FGM.

*2.2. Test specimen preparation*

The final FGM sheets were extracted by pulling them from the mold. Then, the samples were cut to standard specimen dimensions with three replicates for each test according to the standard specifications in Table 2 to create the final specimen using a CNC/router machine, as depicted in Figure 3.

**Table 2.** Standard-sized specimens.

| Test item | Specification of test specimen | Standard code |
|---|---|---|
| Tensile | | ASTM D638-02a |
| Flexural | | ASTM D790 & ISO 178 |
| Impact | | ASTM D4812 & ISO 180/U |
| Thermal | | ASTM C518–02 |
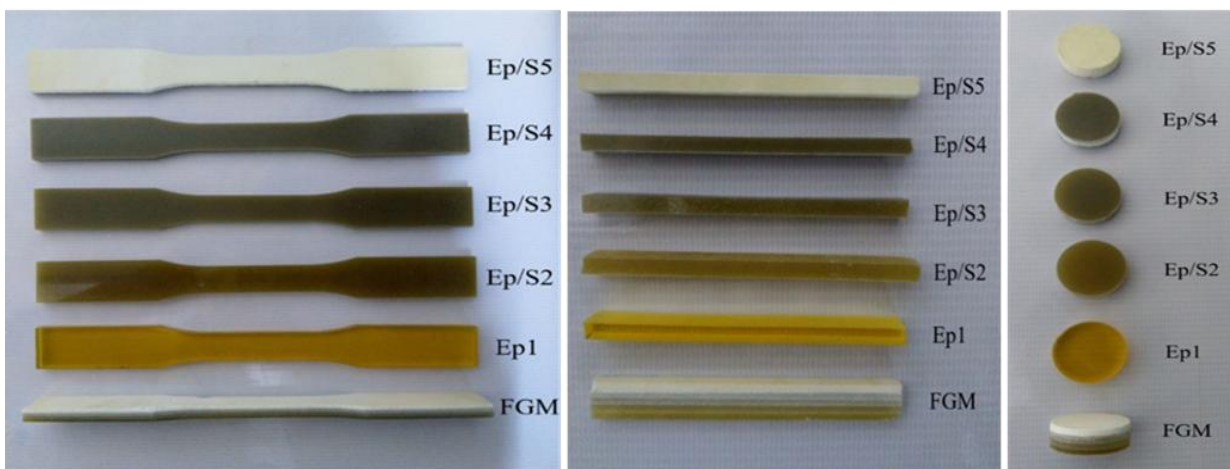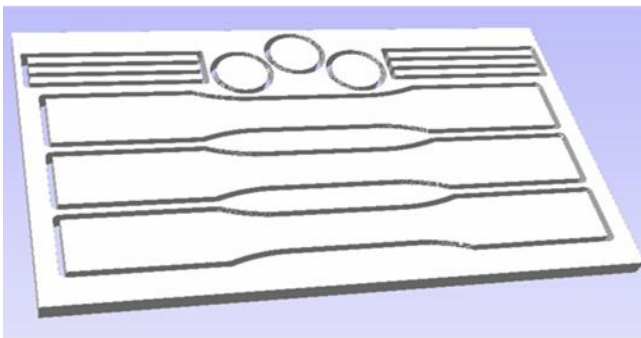


**Figure 3.** Preparing the specimens according to the standard dimensions.

## 3. Experiments

### 3.1. X-ray diffraction (XRD)

An X-ray diffraction (XRD) diffractometer equipped with Fe-K alpha radiation was used to explore the microstructure, analyze the distribution of silica particles within the epoxy matrix, and evaluate the miscibility of the silicon dioxide in epoxy resin at the fractured surfaces of the FGM specimen across a 2 range of 10–60 °at a scanning rate of 2 s per step and a step size of 0.02 °.

### 3.2. Infrared spectroscopy

Infrared spectroscopy (IR) was utilized to verify the surface morphology of the silica fillers within the polymer matrix. In this study, the typical examined spectroscopy transmission spectra of the neat epoxy surface and epoxy-silica surface were analyzed. A small portion of the FGM specimen was ground and molded into a typical pellet for FT-IR study in the transmission mode. The scan range was medium: from 4000 to 400 $cm^{-1}$.

### 3.3. Density

The density of the composite was determined using ASTM standard D792-08 via Eq 1. All samples were weighed using an accurate electronic scale to within 0.01 g of accuracy.

$$\rho = m/v \tag{1}$$

where $\rho$ is the density of the composite, $kg/m^3$; $m$ is the mass of the material, kg; $v$ is the volume, $m^3$.

### 3.4. Mechanical properties

The FGM specimen and layer specimen composites Ep1, Ep/S2, Ep/S3, Ep/S4, and Ep/S5 were subjected to tensile, bending, and impact testing, as explained in the following subsections.

#### 3.4.1. Tensile test

Tensile testing of the material specimens was conducted on an industrial universal testing machine—DX-C4A-G7F Model-Instron—in accordance with the ASTM D638-02a standard. These specimens were loaded to failure at a constant rate of 5 mm/min. On the Instron's x-y recorder, a direct plot of the stress-strain curve for each specimen tested was obtained. A modulus of elasticity plot of the five gradient layers of the FGM specimen was computed using Eq 2:

$$E = \Delta\sigma/\Delta\epsilon \tag{2}$$

where E is the modulus of elasticity in tensile, MPa; $\Delta\sigma$ is the stress change, MPa; $\Delta\epsilon$ is the strain change, mm/mm.

### 3.4.2.   Flexural test

A WDW-5E electronic universal testing machine, which had a 5-kN full-scale load, was used to conduct a bending test on the material specimens. According to ASTM D790, the three-point test was used as the flexural test in this study. At a rate of 0.5 mm/min, the load was applied until a rupture occurred. The x-y recorder of the electronic universal testing machine was used to obtain a direct plot of the stress-strain curve for each tested specimen.

### 3.4.3.   Impact test

An impact test was conducted with a Pendulum Wp 400 impact testing equipment in accordance with ASTM D4812 and ISO 180U on the unnotched beam impact resistance. For each tested specimen, impact work results were obtained; the direction of the impact striker was on the 10-mm-wide face of the test specimen. Equation 3 was used to determine the impact strength:

$$I_s = I_w/A \tag{3}$$

where $I_s$ is the impact strength, J/mm$^2$; $I_w$ is the impact energy, J; A is the cross-sectional area of the specimen, mm$^2$.

### 3.5. Thermal properties

The measured thermal characteristics in this work were based on Lee's disk technique in accordance with ASTM C518-02. The thermal conductivity of each specimen was computed using Eq 4 [25,26]:

$$K = mc_p[(dT/dt)d/A(T2 − T1)] \tag{4}$$

where K is the thermal conductivity, W/m·°C; m is the mass of the brass disk, kg; $c_p$ is the specific heat capacity, J/kg·°C; $dT/dt$ is the rate of cooling of the brass disk at a steady-state temperature, °C/s; d is the thickness of the specimen, mm; A is the cross-sectional area, mm$^2$; (T2 − T1) is the temperature difference across the material's thickness, °C.

## 4.   Results and discussion

### 4.1. Sample characterization

The XRD of the FGM sample in Figure 4 revealed silica particles in the epoxy. The SiO$_2$ peaks appeared in the diffuse analysis as a sharp peak at 25°–30°, which was indicative of the phases of silica included in the material. However, in certain regions of the matrix, little particle clustering was detected. Compared to the standard silica test, this result clearly demonstrates that silica particles were strongly bonded to the epoxy matrix via physical bonding, and there was no chemical reaction with other components, as explained by Daramola et al. [27]. In addition, infrared spectroscopy (IR) examinations of the FGM layers indicated that the compositions of silica particles and epoxy had a strong association with their physical structures. Figure 5 depicts the FTIR spectra of epoxy resin and epoxy containing silica (SiO$_2$). The epoxy spectrum clearly shows the presence of epoxide rings

(characteristic peaks) at 862 and 914 cm$^{-1}$. The peaks at 1033.49 cm$^{-1}$ and 1110.99 cm$^{-1}$ were due to the symmetrical aromatic C–O stretching and asymmetrical aliphatic C–O stretching, respectively. In contrast, asymmetrical aromatic C–O stretching appeared at 1242.15 cm$^{-1}$. At 1296.24 cm$^{-1}$, the vibration mode of the asymmetrical CH$_2$ deformation occurred. The C-C stretching vibrations in the aromatic ring appeared at 1465.9 cm$^{-1}$ to 1612.49 cm$^{-1}$. The symmetrical stretching of C–H from the CH$_3$ group appeared at 2854.64 cm$^{-1}$, while the asymmetrical stretching of C–H from the CH$_2$ group appeared at 2926.7 cm$^{-1}$, which is consistent with the work of Sipaut et al. [28]. Nonetheless, in the epoxy-silica spectrum, there was clear evidence of the presence of silica in this composite, where some peaks were broader than their initial areas. For instance, the broad peak from 1060–1220 cm$^{-1}$ is due to the aromatic and aliphatic C–O stretching from epoxy and the vibration of Si–O from silica. Additionally, the band at 798.8 cm$^{-1}$ is due to the C–O stretching from epoxy and vibration of O–Si–O from silica, which is consistent with Kim et al. [29].
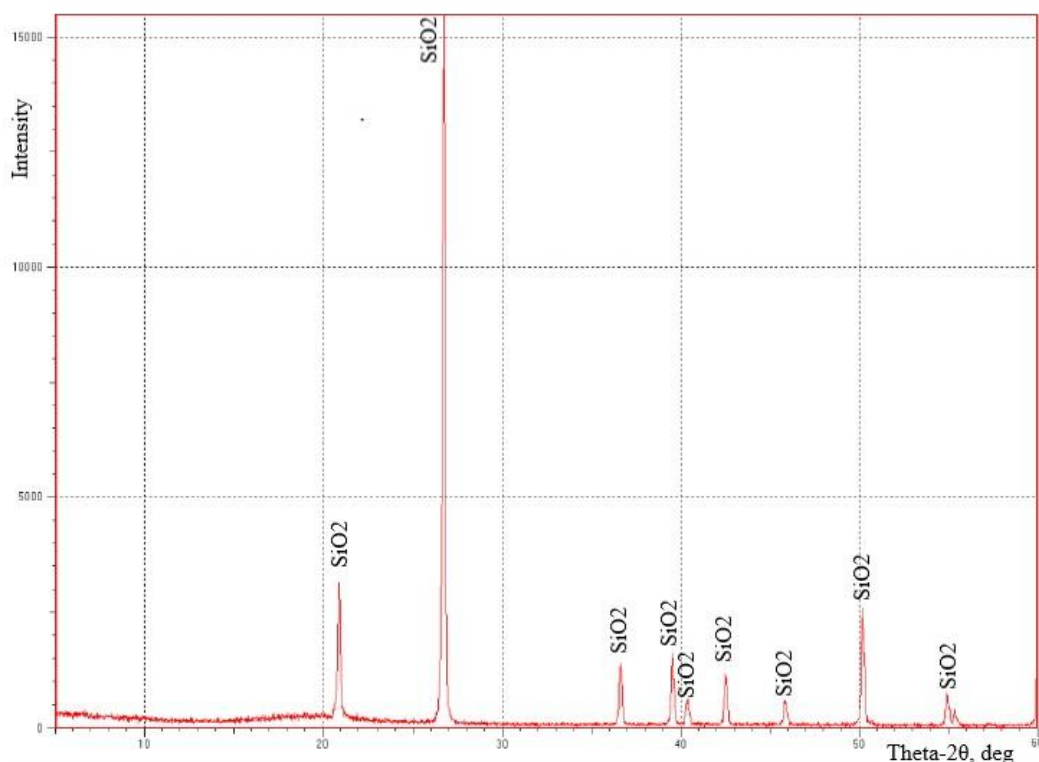


**Figure 4.** Spectrometric profile of epoxy-SiO$_2$ FGM specimen.
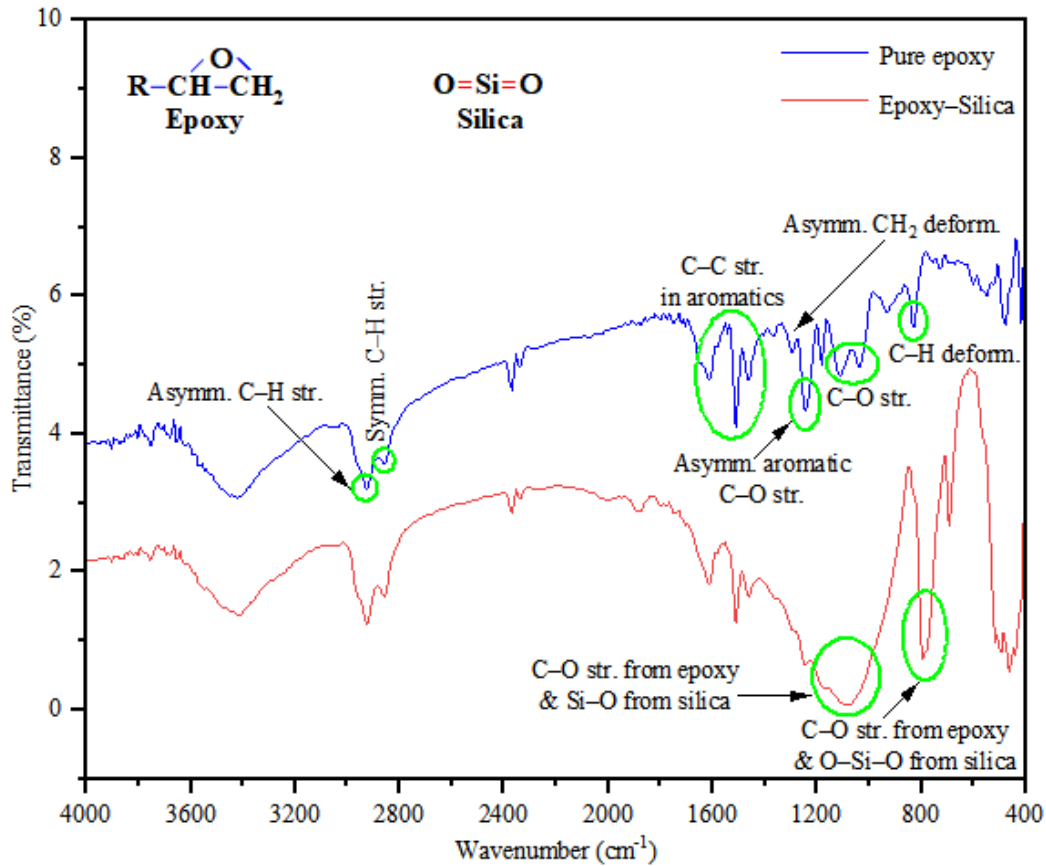
**Figure 5. FT**IR spectra of epoxy and epoxy-silica FGMs.

## 4.2. Density

Figure 6 depicts the density of every layer of the FGM. The addition of silicon dioxide increased the density of the polymer composite because silica has a higher density than epoxy, and the silica particles reduced the porosity of the composites, which is consistent with the work of Misra et al. [30]. When the ratio of silica particles increased, the porosity decreased [31]. Therefore, the density of the samples in the epoxy matrix groups was directly proportional to the ratio of silicon dioxide. When the porosity of the polymer composite diminished, its structure became denser and reached a maximum at 80 wt%, which was 20.95% higher than that of the pure epoxy. The density of the FGM specimen increased by 10.67% on average compared to the density of neat epoxy.
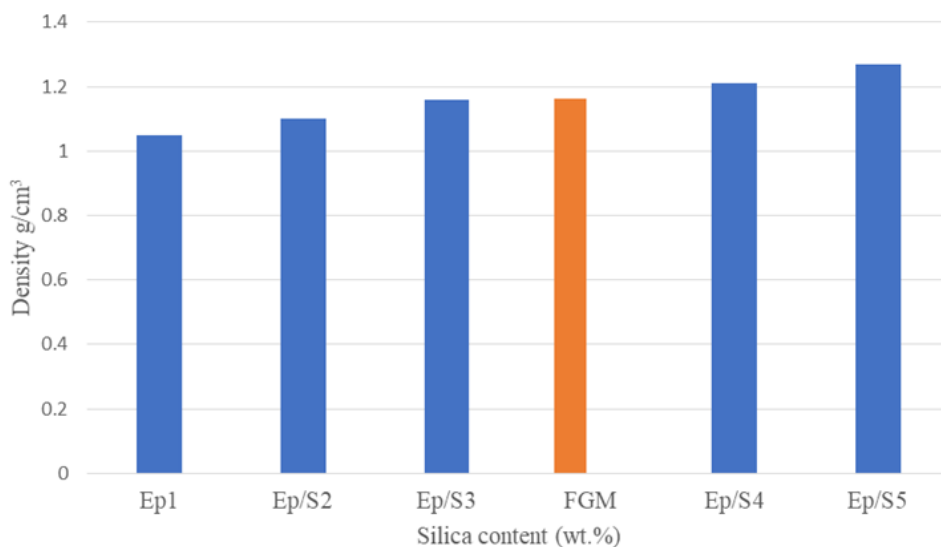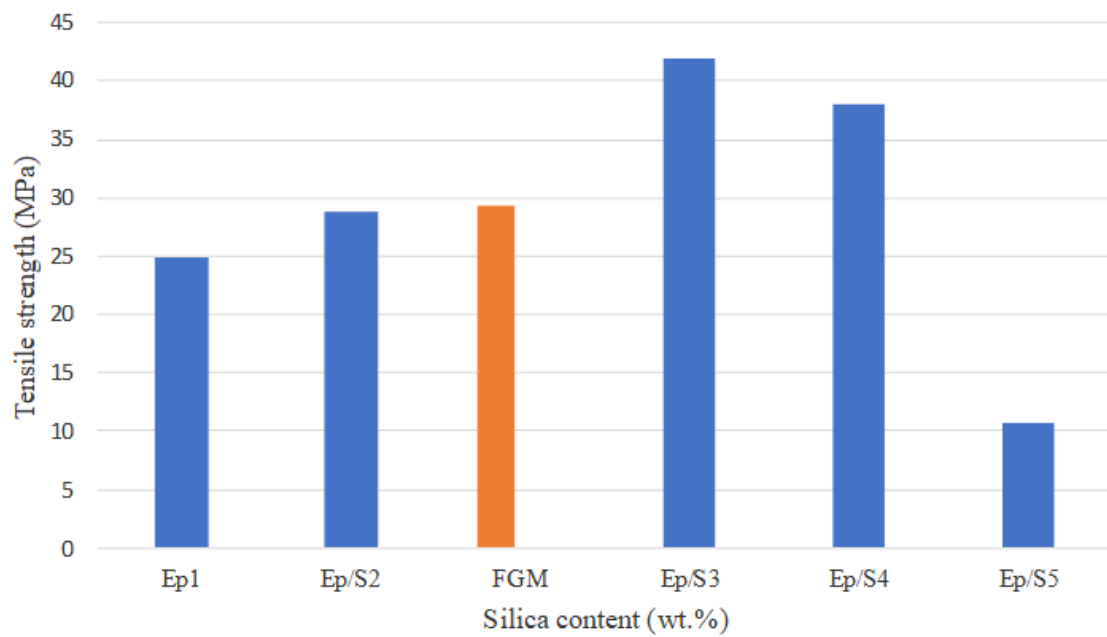
**Figure 6.** Density of epoxy-SiO$_2$ composites for each layer and the FGM specimen.

### 4.3. Tensile test

Figure 7 depicts the tensile stress-strain curve of the FGM specimen. The ultimate tensile strength obtained (29,625 MPa) is the highest stress that a specimen can bear while being pulled before breaking. Figure 8 illustrates the increase in tensile strength of the five layers of the FGM specimen with the increase in silicon dioxide loading from 0% to 60%. The Ep/S3 specimen with 40% SiO$_2$ had the maximum tensile strength (41.9 MPa). The improved tensile strength with SiO$_2$ wt% loading may have been due to the quantity of silica particles and the strong interfacial interaction between reinforcement and matrix, which reduced rapid fracture propagation and enhanced the stress transfer, as reported by Chen et al. [32]. All specimens examined obeyed Hooke's law, which provided data on the modulus of elasticity of the composite. Figure 9 illustrates that all generated composite specimens had higher moduli than the pure epoxy specimen, which is consistent with the work of Yusra et al. [33], the elastic modulus significantly increased because silica has a greater modulus than epoxy, since hard, dispersed phases have higher stiffness than the matrix material. The substantial decrease in tensile strength values at 80 wt% SiO$_2$ can be attributed to the decrease in cross-link density generated by increasing the silica particles, which resulted in the decreased tensile strength of specimen Ep/S5. However, the decrease in tensile strength improved the elastic modulus, which is consistent with the work of Vikram et al. [34]. The enhanced FGM value played a significant role in enhancing the tensile strength and elastic modulus, since it was determined to be of average magnitude and significance.
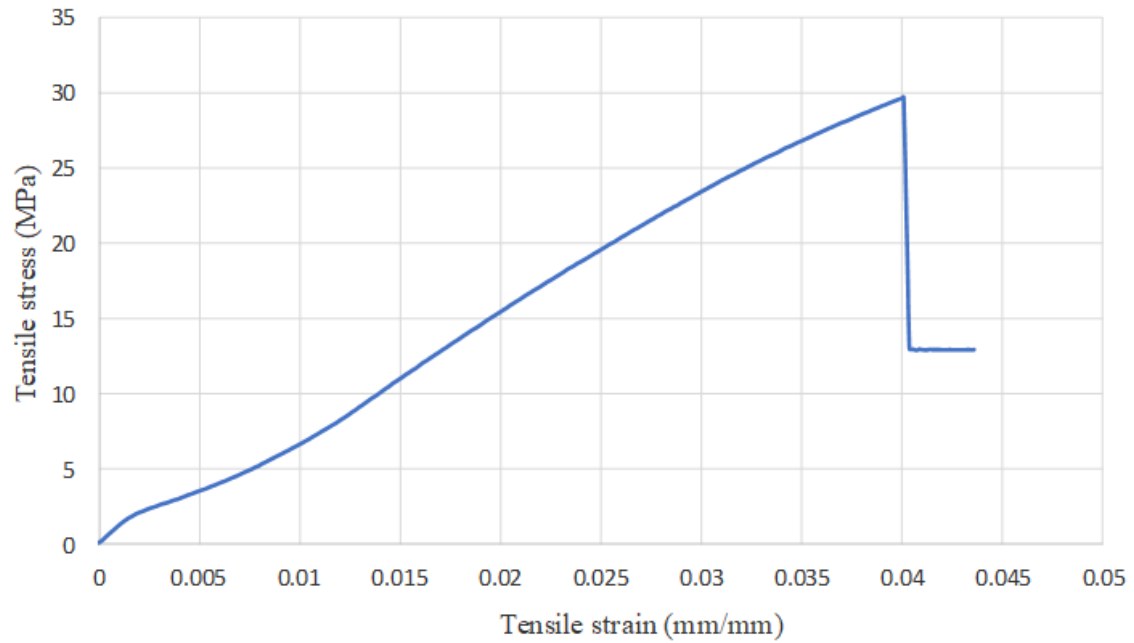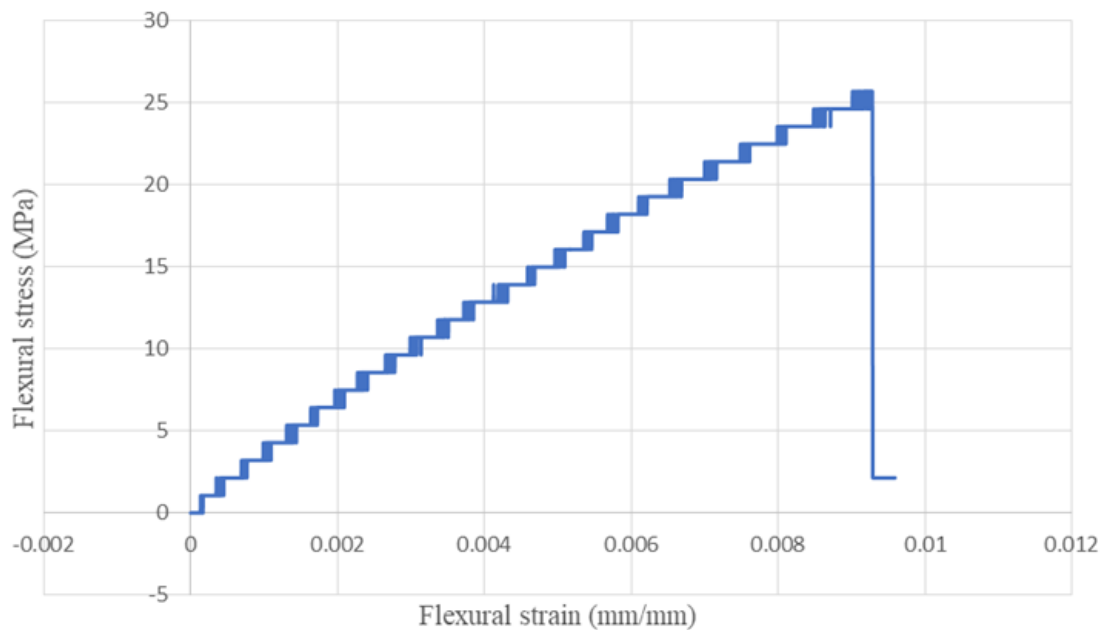
**Figure 7.** Tensile stress-strain of the FGM specimen.



**Figure 8.** Tensile strength of epoxy-SiO$_2$ composites for each layer and the FGM specimen.
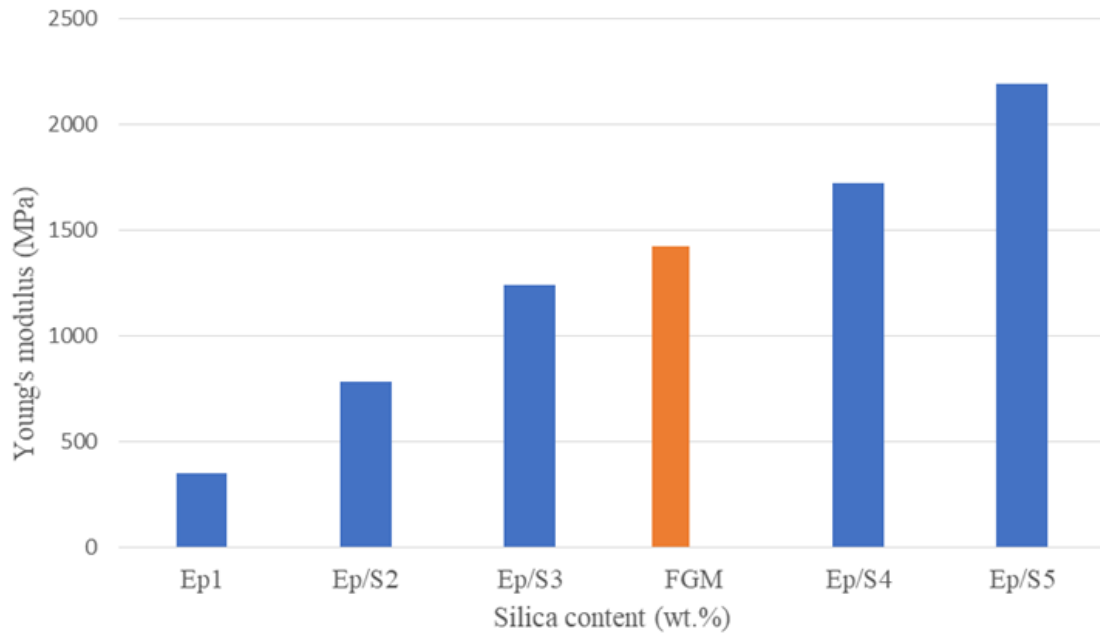
**Figure 9.** Young's modulus of epoxy-SiO$_2$ composites for each layer and the FGM specimen.

## 4.4. Flexural test

According to the stress-strain curve in Figure 10, the flexural strength of the FGM was 25.71 MPa. As depicted in Figure 11, the flexural strength of the five layers of FGM gradually increased from 19.59 to 35.88 MPa from Ep1 to Ep/S3 in the composite reinforced with 40% silicon dioxide.



**Figure 10.** Flexural stress-strain for the FGM specimen.

The increased flexural strength of the epoxy-silica composites was attributed to the interfacial adhesion between epoxy and dispersed silica particles, which limited the mobility of the matrix under further loading, according Jae Jun's report [35]. The lower flexural strength of the Ep/S5-reinforced composite compared to the Ep/S3 composite was caused by an increase in nonstick interface between resin and filler due to a higher silica particle loading percentage, based on Joo Eon et al. [36].
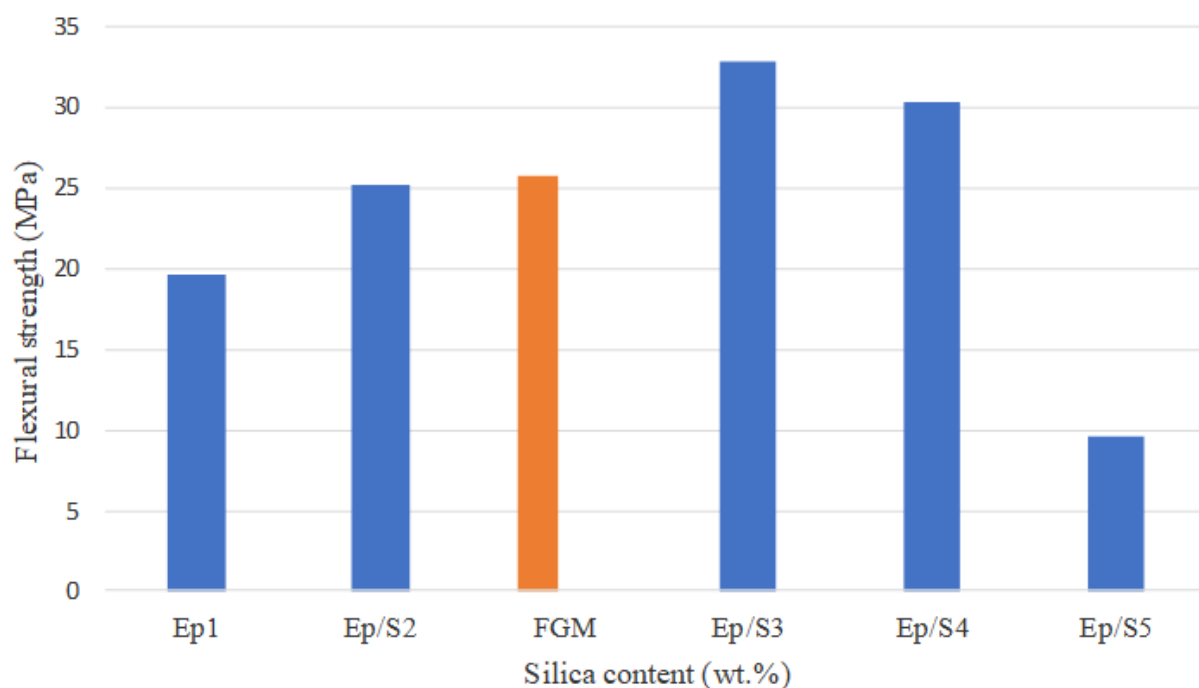


**Figure 11.** Flexural strength of epoxy-SiO$_2$ composites for each layer and the FGM specimen.

### 4.5. Impact test

Equation 4 was used to calculate the impact strength of the FGM composite, which was found to be 4,028 J/m$^2$. Figure 12 illustrates that the impact strengths of the five layers of the FGM composites revealed a slight improvement at the Ep/S2 and Ep/S3 content ratios. The Ep/S4 specimen had the highest impact strength, which decreased in the Ep/S5 specimen due to its larger concentration of silica particles. Reinforcement enhances the impact strength and fracture toughness, which highly depend on the filler volume content. Furthermore, the use of silica particles improves the impact resistance, as shown by Umit et al. [37]. The weak borders of specimen Ep/S5 may be due to the effect of the silica particle concentration on the homogeneity of the epoxy network's crosslinking according to Alameri and Oltulu [38].

### 4.6. Thermal properties

The effects of the silica filler on the thermal conductivity of composites loaded with silica particles are depicted in Figure 13. The measured thermal conductivity of all investigated composites increased when the filler loading increased. Comparing the FGM specimen to the epoxy-silica

composites, the FGM specimen had a thermal conductivity of 0.37 W/m ·°C. At each filler loading, the composite loaded with a high filler content had a greater thermal conductivity than that with a low filler content. The increase in thermal conductivity can be attributed to an improved bonding between the particles and the matrix. These increases are comparable to those reported by Poh et al. [39].
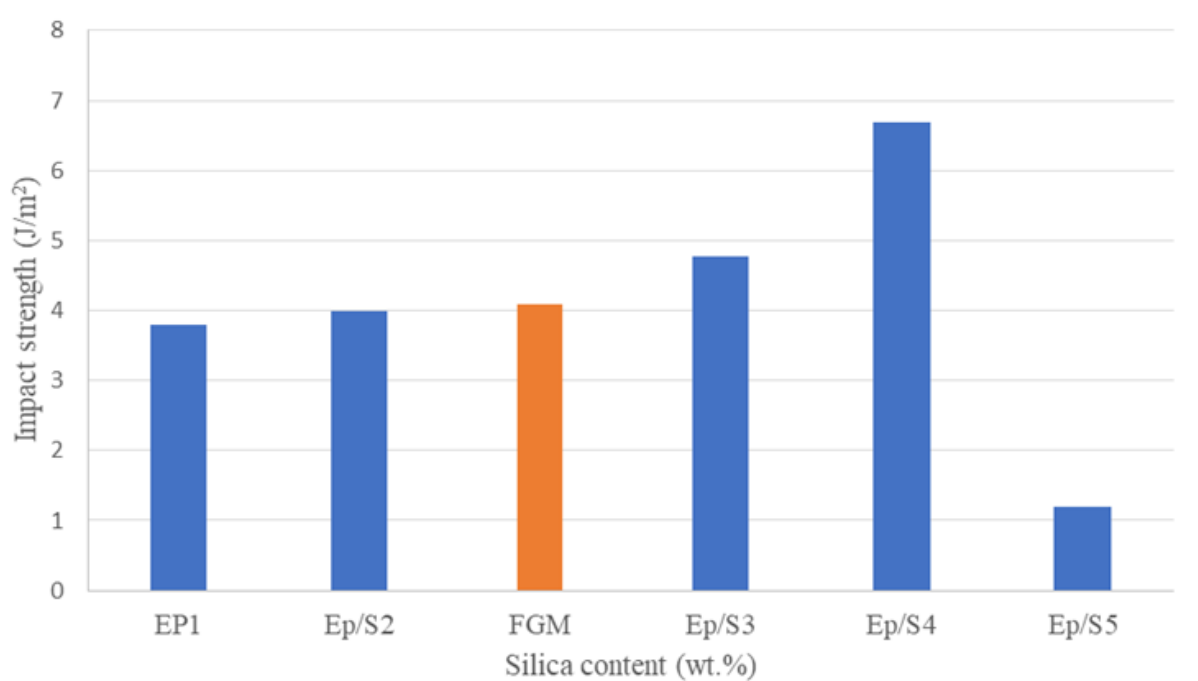


**Figure 12.** Impact strength of epoxy-SiO$_2$ composites for each layer and the FGM specimen.
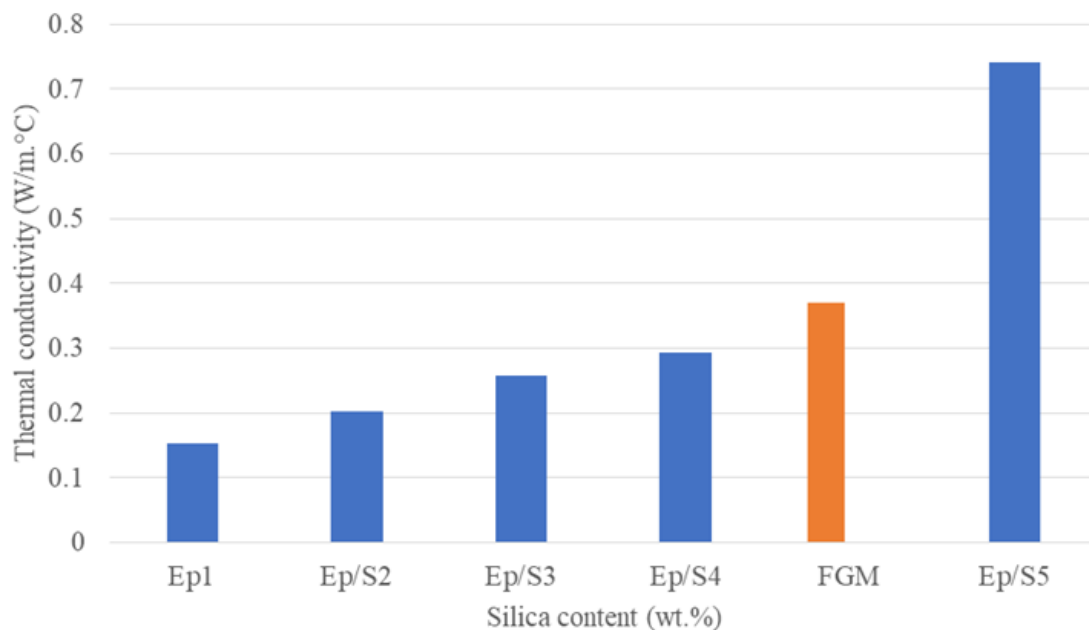


**Figure 13.** Thermal conductivity of epoxy-SiO$_2$ composites for each layer and the FGM specimen.

## 5. Conclusions

This study examined the effect of silicon dioxide on epoxy composites subjected to tests of tensile, flexural, and impact strengths and thermal conductivity. FGMs with silica-reinforced epoxy composites were created with weight percentages of 0, 20, 40, 60, and 80. Based on the findings of this investigation, the following conclusions were drawn:

(1) The XRD and IR of silicon dioxide-reinforced epoxy composites revealed homogeneous silica particle dispersion in the epoxy. Silica particles were attached to the epoxy matrix via a strong physical association, and the silica did not interact with the epoxy. Therefore, the compatibility of the polymer and silica significantly affected the mechanical and thermal properties of gradient materials for epoxy-silica compositions.

(2) The density increased when the ratio of silicon dioxide increased, with the maximal value being achieved at 80 wt%. Adding silica particles to epoxy as a control element increased the density by 4.8–20.95% compared to pure epoxy. The FGM specimen reinforced with silica gradients was 10.66% denser than pure epoxy.

(3) The addition of silicon dioxide to the epoxy composite increased the tensile and flexural strength for all groups when the silica particle loading increased from 0% to 60%. The optimal proportion of silica was 40%. The ultimate tensile strength of the FGM specimen was 29,625 MPa and its flexural strength was 25.71 MPa, which are 17.68% and 31.18% greater than the tensile and flexural strengths of pure epoxy, respectively.

(4) The modulus nearly linearly increased when the level of added silica particles increased. The FGM specimen was 306.67% greater than the pure epoxy specimen, while the composite with 80 wt% silica had the highest elastic modulus, which was significantly greater than that of pure epoxy.

(5) The impact strength of the gradient materials slightly increased when the ratio of silica increased from 20 to 40 weight percent and thereafter. The maximal significant increase was observed with 60% silica, followed by a decrease due to the effect of the silica particle concentration on the homogeneity of the epoxy crosslinking. Meanwhile, the impact strength of the FGM specimen was 7.71% higher than that of the epoxy specimen.

(6) The highest thermal conductivity of the composites was found when 80 wt% silica particles were utilized. Additionally, it was discovered that the thermal conductivity increased when the filler content increased. Compared to the epoxy-silica composites, the unfilled epoxy resin had a lower thermal conductivity. The FGM specimen had a 141.83% higher thermal conductivity than the pure epoxy specimen.

## Conflict of Interest

The authors confirm that the content of this article has no conflicts of interest.

## References

1. Jahromi BH, Ajdari A, Nayeb-Hashemi H, et al. (2010) Autofrettage of layered and functionally graded metal-ceramic composite vessels. *Compos Struct* 92: 1813–1822. https://doi.org/10.1016/J.COMPSTRUCT.2010.01.019

2.  Abood AM, Khazal H, Hassan AF (2021) On the determination of first-mode stress intensity factors and T-stress in a continuous functionally graded beam using digital image correlation method. *AIMS Mater Sci* 9: 56–70. https://doi.org/10.1016/j.matpr.2021.02.768

3.  Willert-Porada M (2010) Design and fabrication strategy in the world of functional gradation. *Int J Mater Prod Technol* 39: 59–71. https://doi.org/10.1504/IJMPT.2010.034260

4.  Bondioli F, Cannillo V, Fabbri E, et al. (2006) Preparation and characterization of epoxy resins filled with submicron spherical zirconia particles. *Polimery* 51: 794–798. https://doi.org/10.14314/polimery.2006.794

5.  Haque ZU, Turner DT (1987) Influence of particulate fillers on the indentation hardness of a glassy cross-linked polymer. *J Mater Sci* 22: 3379–3384. https://doi.org/10.1007/BF01161208

6.  Conradi M (2013) Nanosilica-reinforced polymer composites. *Mater Tehnol* 3: 285–293. Available from: http://www.dlib.si/?URN=URN:NBN:SI:doc-KHZVVWFD

7.  Phong NT, Gabr MH, Anh LH, et al. (2013) Improved fracture toughness and fatigue life of carbon fiber reinforced epoxy composite due to incorporation of rubber nanoparticles. *J Mater Sci* 48: 6039–6047. https://doi.org/10.1007/s10853-013-7400-z

8.  Schmidt D, Shah D, Giannelis EP (2002) New advances in polymer/layered silicate nanocomposites. *Curr Opin Solid State Mater Sci* 6: 205–212. https://doi.org/10.1016/S1359-0286(02)00049-9

9.  Shen M, Bever MB (1972) Gradients in polymeric materials. *J Mater Sci* 7: 741–746. https://doi.org/10.1007/BF00549902

10. Woldemariam MH, Belingardi G, Koricho EG, et al. (2019) Effects of nanomaterials and particles on mechanical properties and fracture toughness of composite materials: a short review. *AIMS Mater Sci* 6: 1191–1212. https://doi.org/10.3934/matersci.2019.6.1191

11. Hassan AF, Abood AM, Khalaf HI, et al. (2022) A review of functionally graded materials including their manufacture and applications. *Int J Mech Eng* 7: 744–755. https://doi.org/10.21203/rs.3.rs-1936049/v1

12. Chmielewski M, Pietrzak K (2016) Metal-ceramic functionally graded materials - manufacturing, characterization, application. *Bull Polish Acad Sci Tech Sci* 64: 151–160. https://doi.org/10.1515/bpasts-2016-0017

13. Hadj Mostefa A, Merdaci S, Mahmoudi N (2018) An overview of functionally graded materials «FGM». *SMSD* 267–278. https://doi.org/10.1007/978-3-319-89707-3_30

14. Araki N, Tang DW, Ohtani A (2006) Evaluation of thermophysical properties of functionally graded materials. *Int J Thermophys* 27: 209–219. https://doi.org/10.1007/S10765-006-0034-5

15. El-Galy IM, Saleh BI, Ahmed MH (2019) Functionally graded materials classifications and development trends from industrial point of view. *SN Appl Sci* 1: 1–23. https://doi.org/10.1007/S42452-019-1413-4

16. Gasik MM (2010) Functionally Graded Materials: Bulk processing techniques. *Int J Mater Prod Technol* 39: 20–29. https://doi.org/10.1504/IJMPT.2010.034257

17. Park JJ, Yoon KG, Lee JY (2011) Thermal and mechanical properties of epoxy/micro- and nano-mixed silica composites for insulation materials of heavy electric equipment. *Trans Electr Electron Mater* 12: 98–101. https://doi.org/10.4313/TEEM.2011.12.3.98

18. Farouq W, Khazal H, Hassan AKF, (2019) Fracture analysis of functionally graded material using digital image correlation technique and extended element-free Galerkin method. *Opt Lasers Eng* 121: 307–322. https://doi.org/10.1016/j.optlaseng.2019.04.021

19. Migliaresi C, Pegoretti A (2002) Fundamentals of polymeric composite materials. *Integr Biomater Sci* 69–117. https://doi.org/10.1007/0-306-47583-9_3

20. Linec M, Mušič B (2019) The effects of silica-based fillers on the properties of epoxy molding compounds. *Materials (Basel)* 12: 1–11. https://doi.org/10.3390/ma12111811

21. Al-Ajaj EA, Alguraby AS, Jawad MK (2015) Nano-SiO$_2$ addition effect on flexural stress and hardness of EP/MWCNT. *Eng Tech J* 33: 1248–1257. Available from: https://etj.uotechnology.edu.iq/article_116689.html.

22. Rihan Y, Abd El-Bary B (2012) Wear resistance and electrical properties of functionally graded epoxy-resin/silica composites. *International Atomic Energy Agency (IAEA)* 44: 23–27. Available from: https://inis.iaea.org/search/search.aspx?orig_q=RN:44066233.

23. Muslim NB, Hamzah AF, Al-kawaz AE, (2018) Study of mechanical properties of wollastonite filled epoxy functionally graded composite. *Int J Mech Eng Technol* 9: 669–677. Available from: http://repository.uobabylon.edu.iq/papers/publication.aspx?pubid=18509.

24. Parihar RS, Setti SG, Sahu RK (2018) Recent advances in the manufacturing processes of functionally graded materials: A review. *Sci Eng Compos Mater* 25: 309–336. https://doi.org/10.1515/secm-2015-0395

25. Sombatsompop N, Wood AK (1997) Measurement of thermal conductivity of polymers using an improved Lee's Disc apparatus. *Polym Test* 16: 203–223. https://doi.org/10.1016/S0142-9418(96)00043-8

26. Pandey A, Kattamuri PK, Sastry BS (2021) Measurement of thermal conductivity of sandstone using Lee's apparatus: A case study. *Mining Metall Explor* 38: 1997–2003. https://doi.org/10.1007/s42461-021-00461-4

27. Daramola OO, Akintayo O (2017) Mechanical properties of epoxy matrix composites reinforced with green silica particles. *Ann Fac Eng Hunedoara-Int J Eng* 4: 167–174. Available from: https://www.researchgate.net/publication/327551546.

28. Sipaut CS, Ahmad N, Adnan R, et al. (2007) Properties and morphology of bulk epoxy composites filled with modified fumed silica-epoxy nanocomposites. *J Appl Sci* 7: 27–34. https://doi.org/10.1002/jrs.1315

29. Kim D, Chung I, Kim G (2014) Study on mechanical and thermal properties of fiber-reinforced epoxy/hybrid-silica composite. *Fibers Polym* 14: 2141–2147. https://doi.org/10.1007/s12221-013-2141-9

30. Misra N, Kapusetti G, Pattanayak DK, et al. (2011) Fabrication and characterization of epoxy/silica functionally graded composite material. *Indian J Phys* 85: 1393–1404. https://doi.org/10.1007/s12648-011-0161-0

31. Ahmada T, Mamat O (2012) Tronoh silica sand nanoparticle production and applications design for composites. *Defect Diffus Forum* 330: 39–47. https://doi.org/10.4028/www.scientific.net/DDF.330.39

32. Chen L, Chai S, Liu K, et al. (2012) Enhanced epoxy/silica composites mechanical properties by introducing graphene oxide to the interface. *ACS Appl Mater Interfaces* 4: 4398–4404. https://doi.org/10.1021/am3010576

33. Yusra AFI, Khalil HPSA, Davoudpour Y, et al. (2015) Characterization of plant nanofiber-reinforced epoxy composites. *BioResources* 10: 8268–8280. https://doi.org/10.15376/biores.10.4.8268-8280

34. Vikram Singh V, Jaiswal P, et al. (2021) Mechanical properties of silica fume reinforced epoxy glass microballoons syntactic foams. *Mater Today Proc* 46: 672–676. https://doi.org/10.1016/j.matpr.2020.11.745

35. Park JJ (2018) Mechanical properties of epoxy/micro-silica and epoxy/micro-alumina composites. *Trans Electr Electron Mater* 19: 481–485. https://doi.org/10.1007/s42341-018-0074-0

36. Park J, Park J (2018) Electrical and mechanical strength properties of epoxy/micro silica and alumina composites for power equipment for power equipment. *J Korean Inst Electr Electron Mater Eng* 31: 496–501. https://doi.org/10.4313/JKEM.2018.31.7.496

37. Ozcan UE, Karabork F, Yazman S, et al. (2019) Effect of silica/graphene nanohybrid particles on the mechanical properties of epoxy coatings. *Arab J Sci Eng* 44: 5723–5731. https://doi.org/10.1007/s13369-019-03724-x

38. Alameri I, Oltulu M (2020) Mechanical properties of polymer composites reinforced by silica-based materials of various sizes. *Appl Nanosci* 10: 4087–4102. https://doi.org/10.1007/s13204-020-01516-6

39. Poh CL, Mariatti M, Ahmad Fauzi MN, et al. (2014) Tensile, dielectric, and thermal properties of epoxy composites filled with silica, mica, and calcium carbonate. *J Mater Sci Mater Electron* 25: 2111–2119. https://doi.org/10.1007/s10854-014-1847-9